

# Investigation of CNSL-Based Hybrid Sol in Conventional Polymeric Material

Dinesh Balgude and Anagha Sabnis\*

*Department of Polymer and Surface Engineering, Institute of Chemical Technology, Nathalal Parekh Marg, Matunga (E), Mumbai - 400019, India*

Received September 21, 2015; Accepted November 13, 2015

**ABSTRACT:** The performance properties of conventional polymeric material have been investigated by modifying it with cashew nut shell liquid (CNSL) derived hybrid precursor. The synthesis of hybrid material involved formation of maleic anhydride adduct of CNSL followed by silane modification and subsequent hydrolysis and condensation with tetra ethyl orthosilicate. The developed hybrid material was characterized by a number of instrumental techniques like FT-IR, <sup>1</sup>H-NMR and <sup>13</sup>C-NMR, as reported in our earlier work. In the present work, we have investigated the effect of CNSL-based hybrid material on the performance properties of conventional alkyd-melamine formaldehyde-based stoving system. The synthesized material was used as a modifier at various concentrations (15, 30 and 50 wt% of alkyd resin). The developed coating formulations were applied on mild steel and cured at 120 °C for 30 minutes. Further, the completely cured coatings were evaluated for optical, thermal, mechanical, chemical and solvent resistance properties, hydrolytic stability, UV resistance, corrosion resistance, morphological behavior and elemental distribution properties. The study conducted showed that incorporation of CNSL-based hybrid materials improved overall performance properties by forming crosslinked silane network within the material along with strong metal-oxygen-silicon covalent bond at metal coating interface.

**KEYWORDS:** CNSL, hybrid materials, DSC/TGA, accelerated weathering, SEM/EDAX

## 1 INTRODUCTION

Conventionally metals are protected via surface pretreatment followed by coating applications. In surface pretreatment, chemical conversion coatings have covered the overall market share due to their excellent performance properties, while in coating applications, a number of chemistries have been explored to date, some of them being epoxy, alkyd, polyurethane, phenolic, acrylic, polyester, silicates, etc. [1–11]. In spite of exhibiting excellent properties, the conventional system possesses some serious health, ecological and economical issues [12,13].

One of the possible solutions to these issues can be the use of advanced coating technologies, such as sol-gel chemistry, as an eco-friendly alternative to conventional surface pretreatment, as well as utilization of biomaterials instead of petroleum feedstocks for polymer/resin synthesis. For almost 10 years,

sol-gel derived organic-inorganic hybrid coatings have emerged as an eco-friendly surface protection methodology for metals [14] due to the number of advantages they offer such as room temperature synthesis, chemical inertness, high oxidation and abrasion resistance, excellent thermal stability, very low health hazard, excellent protection against aggressive environment, etc. The hybrid materials are mainly synthesized by acidic/basic hydrolysis and subsequent condensation of organosilane precursors in polar solvents (alcohols, ketone, etc.) via sol-gel process. On application, they offer an excellent adhesion to metals as well as to the subsequent coat via strong covalent bond, while a three-dimensional network of siloxane (–Si–O–Si–) linkages helps to impede the ingress of aggressive chemicals through the coating. The details of various hybrid coatings for metal protection, basic chemistry involved in their synthesis, their interaction with the metal surface and subsequent coat as well, and the current developments in hybrid coatings have been well reported in our previous work [15].

\*Corresponding author: as.sabnis@ictmumbai.edu.in

The increasing worldwide interest in the use of biomaterials is mainly due to the fact that these materials are derived from natural resources which are abundantly available; their use would also contribute to global sustainability without depletion of scarce resources. These biomaterials are usually easily available, more economical and comparatively easy to handle, with no or less toxicity and health-related issues. All these features make biobased materials an attractive topic for academic as well as for industrial research to synthesize polymers/resins for coating industries [16]. The utilization of biobased materials as such or by chemical modifications for various applications, like resin synthesis, adhesives, paints, coatings, composites, etc., has been well reported in the literature [17–23]. Such materials include cellulose, starch, sucrose, sugar, lignin, plant and animal oils, etc. However, there exists a compound like cashew nut shell liquid (CNSL), which can be used as a possible substitute for petroleum-based materials due to its availability, sustainability, cost effectiveness and reactive functionalities.

In our previous work, we have covered the potential of CNSL as an environmentally friendly material for the modern coating industry [24]. Due to its reactive phenolic hydroxyl group and meta substituted unsaturated aliphatic chain, a wide variety of resins can be synthesized from CNSL via addition and/or condensation mechanism. The chemistries being explored using CNSL include alkyd, polyesters, phenolic resins, epoxy resins, polyurethanes, acrylics, vinyl, various curing agents, etc. The present study describes the end-use performance of conventional polymeric materials modified with newly developed CNSL-based hybrid precursor. The detailed studies on the chemical reactions and characterization of developed material have been presented previously [25–27].

## 2 MATERIALS

Cashew nut shell liquid (NC-700) was procured from Cardolite Corporation, Mangalore. 3-glycidyloxypropyl trimethoxysilane (GPTMS) and Tetraethyl orthosilicate (TEOS) were obtained from Wacker Silicones, Mumbai. Maleic Anhydride, anhydrous sodium sulphate ( $\text{Na}_2\text{SO}_4$ ), glacial acetic acid (GAA), methanol, methyl ethyl ketone, xylene, p-toluene sulfonic acid (p-TSA) and triethylamine (TEA) were purchased from SD Fine-Chem Ltd., Mumbai. Short oil alkyd (Replakyd-526) was procured from Resin and Plastics Ltd., Mumbai. Hexabutoxymethylmelamine (HBMM) was obtained from Shalimar Paints Ltd., Nasik, India.

## 3 EXPERIMENTAL

### 3.1 Synthesis of CNSL-Based Hybrid Material

The CNSL-based hybrid material was synthesized by grafting maleic anhydride onto double bond of CNSL via Ene mechanism or by formation of chroman ring via Diels-Alder mechanism, as reported in our earlier work [27]. Conventionally this reaction proceeds radically or thermally. However, undesired curing reaction occurs, unavoidably resulting in gelation of the reaction mixture. The reaction mixture was charged with nitrogen-containing solvent such as n-methyl-2-pyrrolidone (2 wt%) to process the malenization reaction without gelation [28].

After formation of maleic anhydride adduct of CNSL, hydration was carried out by boiling the reaction mixture in water for 1 h to open the anhydride rings. The free carboxylic groups obtained after hydration were then used to modify with silane precursor to incorporate the inorganic moieties in the developed material. The silane modified CNSL-based hybrid material was then processed via sol-gel technology to yield functionally reactive CNSL-based hybrid sol, as shown in Figure 1.

### 3.2 Material Formulation

The synthesized CNSL-based hybrid sol was then used as a modifier in conventional alkyd-melamine formaldehyde (MF)-based stoving system. The curing ratio of alkyd to MF was set at 70:30 wt% respectively. The possible curing reaction is shown in Figure 2. The coating solutions were formulated by replacing alkyd resin with synthesized hybrid sol at 15, 30 and 50 wt% respectively. For comparative study, the neat coating solution was also applied. The modified materials were coded as AM-0, AM-15, AM-30 and AM-50, where AM stands for alkyd-MF resin, while the number denoted as the weight percentage of CNSL-based hybrid sol is a partial replacement of alkyd resin.

### 3.3 Surface Preparation, Material Deposition and Its Curing

Mild steel panels (6 × 4 square inches) were manually cleaned before application. Cleaning involved degreasing, hand scrubbing using emery paper (120 no.) followed by methanol cleaning. The application viscosity of all formulated solutions was maintained at 40% non-volatile matter (%NVM) using a mixture of xylene and methyl ethyl ketone of 90:10 wt%. The formulated solutions were then deposited onto prepared substrate by conventional air-assisted spray application according to

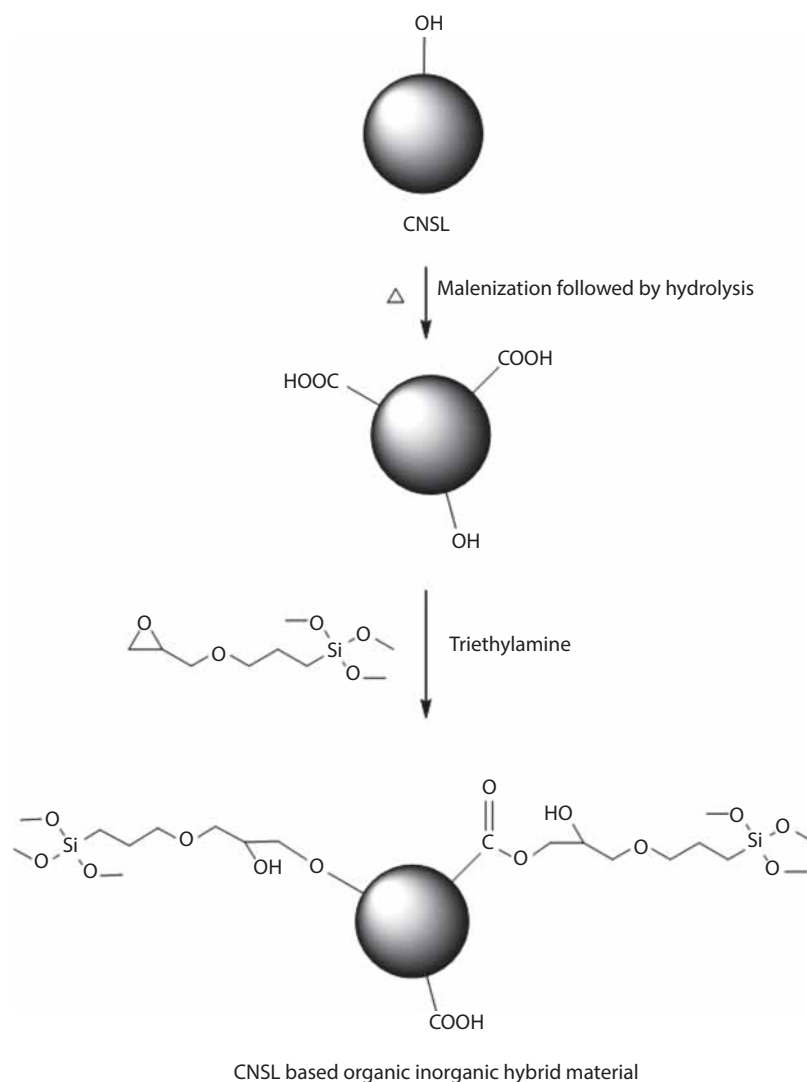


**Figure 1** Schematic representation of synthesis of CNSL-based hybrid sol.

ASTM D 4708-99. The coated panels were kept at room temperature for 10 minutes and were then cured at 120 °C for ½ h. Typical dry-film thickness of cured materials was observed to be in the range of 60–70 microns.

#### 4 METHODS AND MEASUREMENT

The completely cured coatings were characterized by Fourier transform infrared spectroscopy (FTIR) on a MIRacle 10 Shimadzu instrument as per ASTM E-1252. Forty-five scans were recorded for each sample in the spectra range from 4000–500  $\text{cm}^{-1}$ . Further, the formation of siloxane network was evaluated by  $^{29}\text{Si}$ -NMR analysis. The analyses were carried out on a Bruker Biospin (Avance AV500WB, Germany) spectrometer at 400 MHz using deuterated chloroform as solvent and tetramethylsilane (TMS) as an internal standard.

The completely cured materials were tested for adhesion properties by crosscut adhesion method as per ASTM D-3359. Hardness property was evaluated in terms of pencil hardness according to ASTM D-3363. Flexibility and load distribution properties of the materials were tested by conical mandrel and impact tester as per ASTM D-522 and ASTM D-2794 respectively. Impact resistance was measured on the impact tester with maximum height of 60 cm and load of 1.36 kg. The abrasion resistance of the cured materials was evaluated by rotary abraser (CS-17) with 1 Kg load as per ASTM D-4060. The chemical resistance properties of the modified materials were evaluated in terms of their acid and alkali resistances by immersing the coated panels in 5% HCl and 5% NaOH solution according to ASTM D-1308. The film integrity of the modified materials was evaluated by double rub

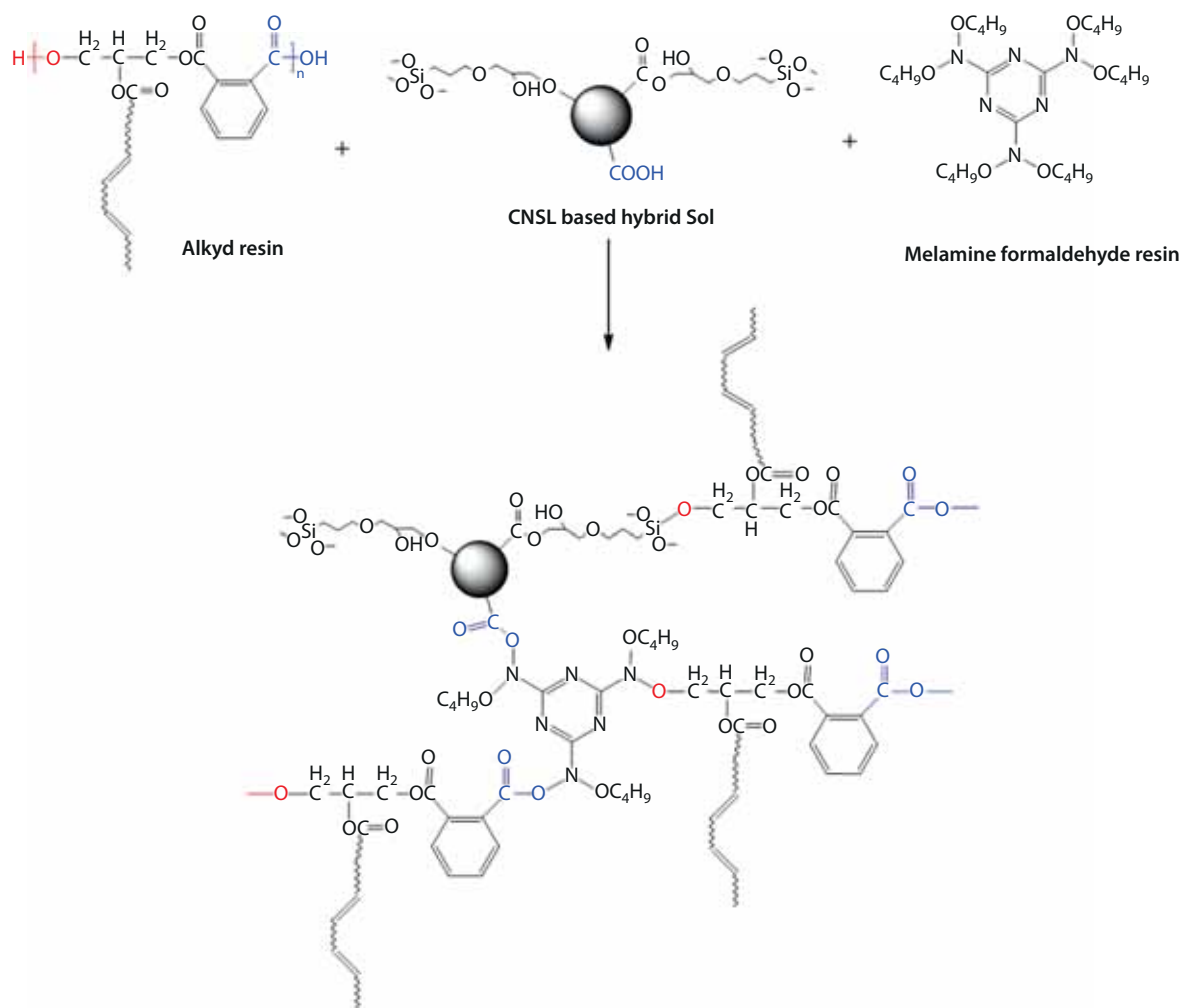


**Figure 2** Curing reaction of CNSL-based hybrid sol in alkyd-melamine formaldehyde system.

method as per ASTM D-4752 using MEK and xylene as solvents.

Thermal behavior was also studied using differential scanning calorimetry (Shimadzu DSC-60) and thermogravimetric analysis (Shimadzu TGA-51) at a heating rate of 10 °C/min under nitrogen atmosphere. DSC was performed by heating the sample from -50 °C to 150 °C at a scan rate of 10 °C/min and a modulated frequency of -0.5 °C every 40 seconds. The test was conducted under a N<sub>2</sub> flow of 10 ml/min. For TGA analysis, samples were evaluated against an alumina standard in a 50 ml/min nitrogen gas flow with temperature ramp of 20 °C/min up to 700 °C.

The performance of the materials against electrolytic environment was evaluated by TAFEL analysis on ACM Instruments Gill AC (Serial No. 1641). The electrochemical studies involved a three-electrode system, namely a saturated calomel electrode, a platinum electrode and a coated panel acting as reference, counter and working electrode respectively. Electrode surface area exposed to testing solution (5 wt% NaCl)

was 1 cm<sup>2</sup> in all the cases. All the electrochemical measurements were recorded at room temperature (32 °C) in 5 wt% NaCl solution.

The surface morphology of cured materials was evaluated by scanning electron microscopy (SEM), whereas elemental distribution was analyzed by energy dispersive spectroscopy (EDAX) using a Quanta 200 SEM instrument (FEI Company, USA). The modified materials were also evaluated for UV resistance (ASTM-G53) to investigate the weatherability properties.

## 5 RESULTS AND DISCUSSION

### 5.1 FTIR and <sup>29</sup>Si-NMR Analysis

The cured materials were evaluated by FTIR analysis to confirm the functional group conversion. Figure 3 shows the FTIR spectra of modified materials containing various percentages of CNSL-based hybrid sol. The graph shows an increase in intensity of peaks at 550

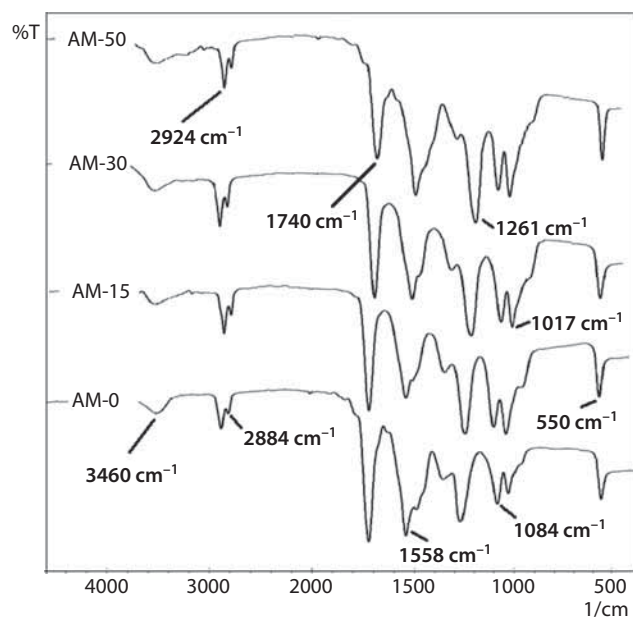


**Figure 3** FTIR spectra of CNSL-based modified hybrid materials.

$\text{cm}^{-1}$ ,  $1017 \text{ cm}^{-1}$ ,  $1084 \text{ cm}^{-1}$  and  $1261 \text{ cm}^{-1}$ , which corresponds to  $-\text{Si}-\text{O}-\text{Fe}-$ ,  $-\text{Si}-\text{O}-\text{CH}_3$  and  $\text{Si}-\text{C}$  [29,30] respectively on increasing the content of hybrid sol. The increased intensity of  $\text{Si}-\text{O}$  stretching in the above-mentioned linkages indicated that the condensation reactions might have occurred between silanol and metal substrate, leading to the formation of a strong covalent bond at metal coating interface. Frequency at  $3460 \text{ cm}^{-1}$  denoted the existence of OH groups. The sharp peaks at  $2924 \text{ cm}^{-1}$  and around  $2884 \text{ cm}^{-1}$  are due to  $-\text{CH}_3$  symmetric stretching and  $\text{O}-\text{CH}_3$  asymmetric stretching vibrations. The significant decrease in the absorption band at  $1740 \text{ cm}^{-1}$  corresponds to  $-\text{C}=\text{O}$  stretching of the ester group, confirming the replacement of alkyd resin by CNSL-based hybrid sol. The peak intensity at  $1558 \text{ cm}^{-1}$  corresponds to  $-\text{C}-\text{N}$  stretching of MF, while the sharp peak at  $1261 \text{ cm}^{-1}$  is attributed to  $\text{Si}-\text{C}$  symmetric bending of  $\text{Si}-\text{CH}_3$  group respectively [31].

The peak assignments in the  $^{29}\text{Si}$ -NMR spectra of hybrid sols are described as previously reported by Glaser *et al.* for organically modified silanes [32]. The spectra (as shown in Figure 4) shows distinct peaks for the silica network units at  $-59.3 \text{ ppm}$  [ $\text{T}^2$ ], and  $-69.9 \text{ ppm}$  [ $\text{T}^3$ ], which corresponds to  $\text{R}-\text{Si}(\text{OR})(-\text{O})_2$ ,  $\text{R}-\text{Si}(\text{O})_3$  respectively. Thus,  $^{29}\text{Si}$ -NMR measurements confirmed the formation of a dense siloxane network evident from increasing peak ratios of  $\text{T}^2/\text{T}^3$  on increasing hybrid sol content (Figure 4). This indicated the enhancement in the degree of condensation in the sol. The increased degree of condensation has led to the formation of higher reticulated network of TEOS and GPTMS in the hybrid material.

## 5.2 Performance Properties

### 5.2.1 Optical and Mechanical Properties

Optical property of the completely cured hybrid materials was evaluated using digital gloss meter at  $60^\circ$ . The gloss values were reported in Table 1. There was no significant difference observed in the gloss values of all the systems.

The crosshatch adhesion as well as flexibility of the modified materials was observed to be excellent (i.e., 5B adhesion and no cracks at 3 mm diameter [acute angle of the conical mandrel]) in all the systems irrespective of the percentage of hybrid sol. The presence of polar functional groups (such as carboxyl and hydroxyl) of hybrid sol would contribute to the strong adhesive forces to the metal substrate, while long methylene linkages of CNSL would take care of any increased crystallinity with increasing silane content, thus contributing to excellent flexibility. However, the pencil hardness was observed to be increased with increasing percentage of hybrid sol, as shown in Figure 5. This could be due to increased surface hardness of the materials on increasing the content of hybrid sol, which resulted in dense crosslinked polymeric network.

The load distribution property of the materials was evaluated by falling ball impact method and it was observed to be increased with increasing concentration of hybrid sol, as shown in Figure 6. The increased number of methylene linkages on increasing the percentage of hybrid sol was responsible for imparting very good flexibility to the systems. The flexibility of the material was adequate to provide excellent load distribution property on impact without any crack development.

Abrasion resistance was observed to follow the similar trend as that of pencil hardness when evaluated for various cycles (500 cycles), as shown in Figure 7. The increased surface hardness of AM-50 formulation due to increased siloxane linkages was responsible for its better abrasion resistance compared to others. The increased crosslink density in the material was balanced by the soft oligomeric segment of hybrid sol, which did not result in any brittleness in the material. Hence the abrasion resistance was observed to be improved as the percentage of hybrid sol increased to 50% (i.e., AM-50).

### 5.2.2 Chemical Resistance Properties

The chemical resistance properties were evaluated by acid and alkali resistance. The coated substrates were dipped in 5% NaOH and 5% HCl solution respectively for 16 h. After completion of the test, panels were inspected visually for damages, if any. The formulation AM-50 showed excellent acid and alkali resistance as

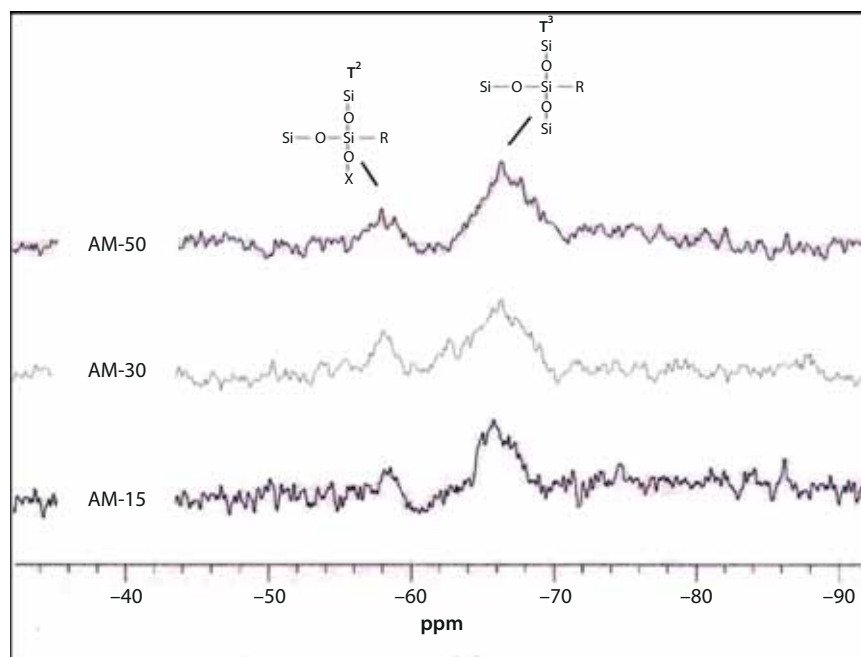


Figure 4  $^{29}\text{Si}$ -NMR of developed hybrid formulations.

Table 1 Performance properties of CNSL hybrid materials.

Properties	AM-0	AM-15	AM-30	AM-50
Dry film thickness (ASTM D-1186)	60–70 $\mu\text{m}$	62–68 $\mu\text{m}$	65–71 $\mu\text{m}$	61–68 $\mu\text{m}$
Gloss (60°) (ASTM D-523)	99–103	100–102	102–105	100–103
Adhesion (ASTM D-3359)				
Primary (at 0 hrs of salt spray exposure)	5B	5B	5B	5B
Secondary (after 300 hrs of salt spray exposure)	3B	4B	5B	5B
Flexibility (ASTM D-522) (Conical mandrel, 3mm diameter)	No crack	No crack	No crack	No crack
Acid Resistance (ASTM D-1308)	Medium dense blisters (Size no. 6)	Medium blisters (Size no. 6)	Few blisters (Size no. 4)	No blisters
Alkali Resistance (ASTM D-1308)	Dense blisters (Size no. 6)	Medium blisters (Size no. 6)	Few blisters (Size no. 4)	No blisters
Solvent Resistance (ASTM D-4752)				
MEK	100 cycles	>200 cycles	>200 cycles	>200 cycles
Xylene	>200 cycles	>200 cycles	>200 cycles	>200 cycles

well. The increased number of siloxane linkages help to impede the ingress of chemicals across the film, thereby imparting excellent chemical resistance irrespective of ester linkages present in the film. However, little blistering was observed in the case of alkali resistance for other materials, which could be due to the presence of ester linkages in the polymeric network which are susceptible to hydrolysis in alkaline environment. The density and size of the blisters were evaluated as per ASTM D-714 and reported in Table 1.

### 5.2.3 Solvent Resistance Properties

The film integrity of the coated panels was evaluated in polar (MEK) and nonpolar (xylene) solvent by double rub method as per ASTM D-4752. After 200 cycles of double rub, the rubbed area was inspected for loss of gloss and degree of softness due to solvent penetration, if any. Among all formulations, AM-30 and AM-50 showed excellent solvent resistance for both MEK and xylene with no loss of gloss. The exposed

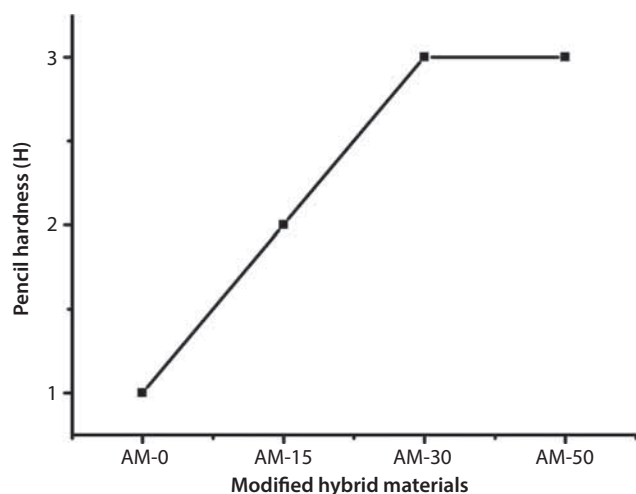


Figure 5 Pencil hardness of modified hybrid materials.

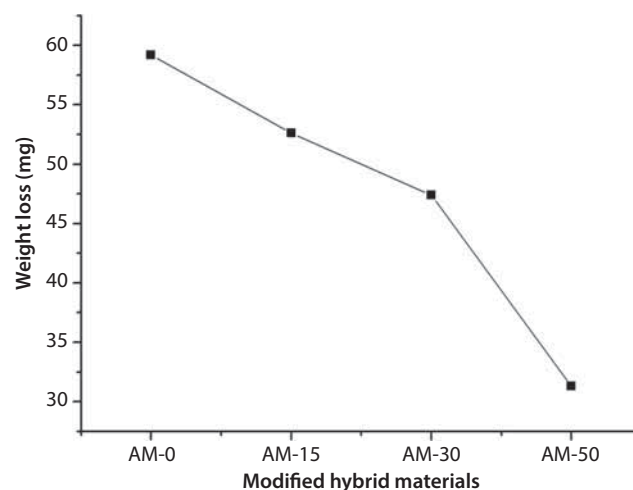


Figure 7 Abrasion resistances of modified hybrid materials.

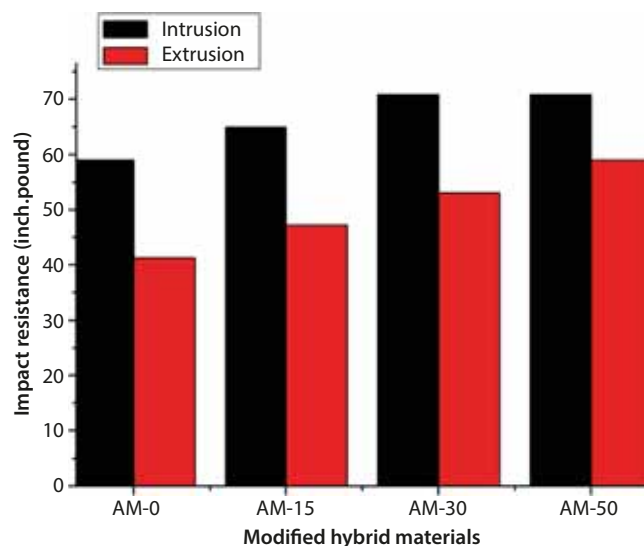


Figure 6 Impact resistances of modified hybrid materials.

area was further evaluated for secondary adhesion and it was observed to be unaffected (i.e., 5B) for both AM-30 and AM-50 formulations. However, formulation AM-0 and AM-15 showed moderate performance with reduced value of secondary adhesion (3B and 4B) and gloss ( $86^\circ$  and  $92^\circ$ ) respectively. The increased quantity of hybrid sol in AM-30 and AM-50 increases the polar functional groups within the coating and therefore increases the adhesive forces with the metal as that of the formulations AM-0 and AM-15.

### 5.2.4 Thermal Properties

The completely cured materials were also evaluated by DSC and TGA to investigate the effect of CNSL-based hybrid sol on the thermal behavior of the alkyd-melamine chemistry. Figure 8 shows a DSC thermograph for CNSL-based hybrid materials. The

glass transition temperature ( $T_g$ ) of the materials was observed to decrease on increasing the concentration of hybrid sol. The increased amount of long aliphatic chain would dominate the effect of an increased amount of crystallinity due to the siloxane network on increasing the hybrid sol concentration.

The TGA plot indicated the relative thermal stability of the modified materials as a function of CNSL-based hybrid sol (inorganic silica content). Figure 9 displays two-stage decomposition. The initial weight loss in the range of  $110\text{--}180^\circ\text{C}$  was probably due to the evaporation of volatile species such as water and alcohol, while the second weight loss was observed to be in the temperature range of  $325\text{--}470^\circ\text{C}$ . This could be due to the thermal decomposition of melamine ring from melamine formaldehyde which undergoes condensation on heating with elimination of ammonia and formation of insoluble products [33]. The temperatures of degradations, i.e., at 10% weight loss ( $T_{d10}$ ), at 50% weight loss ( $T_{50}$ ) and at maximum weight loss ( $T_{max}$ ) were observed to be increased with increasing hybrid sol, i.e., overall silica domain of the CNSL-based hybrid materials, as shown in Figure 9 and Table 2. The TGA study showed that thermal stability of the modified materials improved on increasing the content of CNSL-based hybrid sol. The hybrid material contains a combination of organic and inorganic moieties. As inorganic materials possess better thermal stability than that of the organic material, on increasing the hybrid sol concentration the inorganic content increases, which improves the thermal stability of the coatings.

### 5.2.5 Electrochemical Properties

The electrochemical properties of the modified materials were evaluated by Tafel polarization. From the polarization curves (Figure 10) in the 5% NaCl

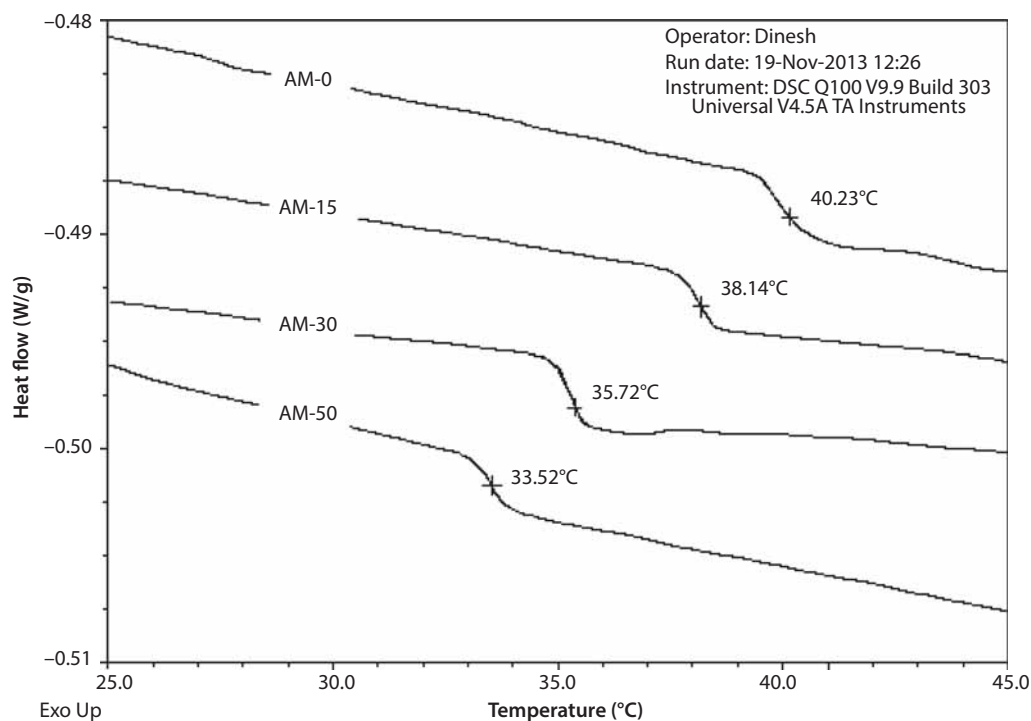


Figure 8 DSC thermographs of modified hybrid materials.

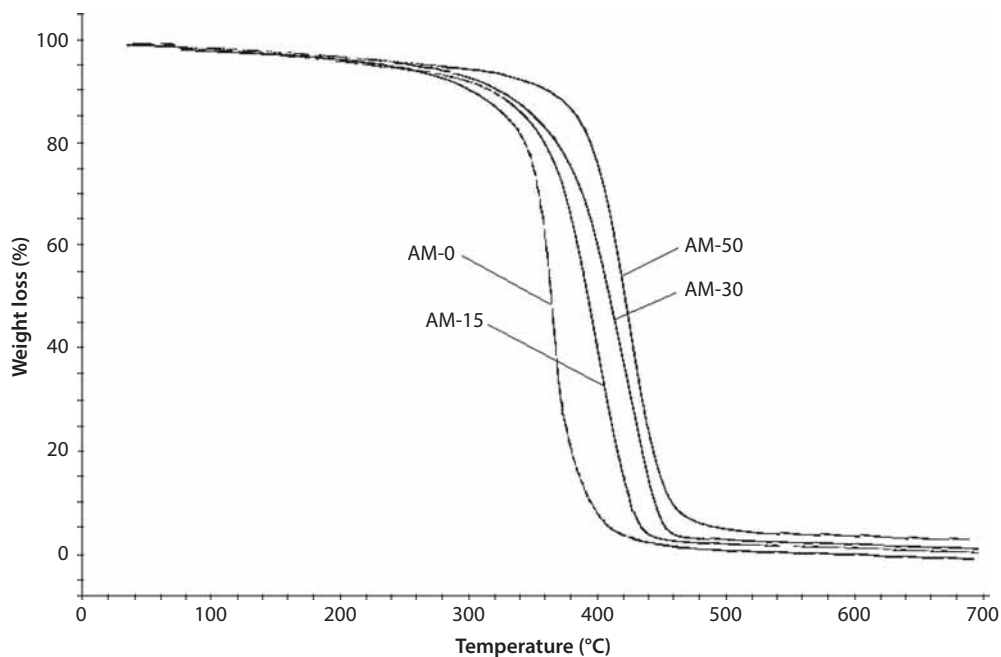
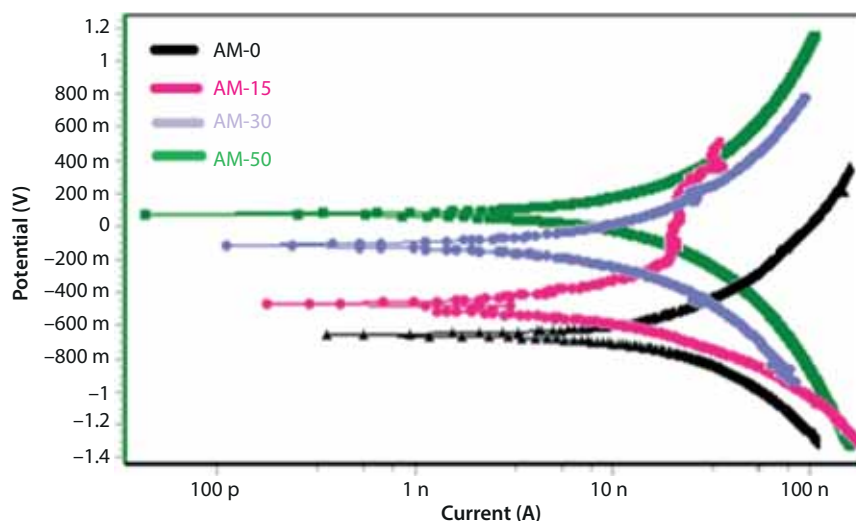


Figure 9 TGA thermographs of modified hybrid materials.

Table 2 Thermal analyses data for CNSL based hybrid materials.

Sample Code	$T_{d10}$ (°C)	$T_{50}$ (°C)	$T_{max}$	Char yield (Wt %)
AM-0	300	365	460	–
AM-15	316	395	465	1.13
AM-30	323	410	480	2.21
AM-50	360	423	505	3.89



**Figure 10** Potentiodynamic polarization curves of CNSL-based modified materials.

**Table 3** Electrochemical parameters for modified hybrid materials.

Formulation	$I_{\text{corr}}$ ( $\mu\text{A}$ )	$E_{\text{corr}}$ (mV)	Corrosion Rate (mm/yr)
AM-0	$1.82 \times 10^{-10}$	-0.725	$5.56 \times 10^{-3}$
AM-15	$2.49 \times 10^{-11}$	-0.516	$3.71 \times 10^{-5}$
AM-30	$7.83 \times 10^{-12}$	-0.150	$1.15 \times 10^{-6}$
AM-50	$5.65 \times 10^{-13}$	-0.087	$8.17 \times 10^{-7}$

solution, it can be seen that the corrosion current for the AM-0 formulation is larger than that of the other formulations. The incorporation of hybrid sol resulted in lower current densities, which showed a continuous decreasing trend with further increase in the content of hybrid sol. The decreased  $I_{\text{corr}}$  ( $\mu\text{A}$ ) values and corrosion rate (mm/yr) (as shown in Table 3) with increasing CNSL-based hybrid sol indicated that more siloxane linkages indeed could provide a physical barrier for blocking the electrochemical process at metal coating interface. Also, Figure 10 shows the highest electrochemical potential (ECP) value for AM-50 formulation. This could be due to the presence of pendant hydroxyl group after hydrolysis which participates in electrochemical reactions through the lone pair of electrons available with oxygen atom in hydroxyl group [34].

### 5.2.6 SEM/EDAX Analysis

The surface morphology of all the modified materials was evaluated by scanning electron microscope using a Quanta 200 SEM instrument (FEI Company, USA). The SEM micrographs revealed that the deposition of

materials on mild steel is uniform, homogenous and crack free. The EDAX graphs show uniformly distributed silica with an increase in area under the peak at 1.739 keV for AM-50 compared to other formulations (as shown in Figure 11). This confirmed the presence of increased silica with increasing content of CNSL-based hybrid sol.

### 5.2.7 UV Resistance Properties

The UV resistance of the coated specimen was evaluated by exposing the coated panels to alternate 4-h cycles of UV light and 4 h of water condensation for 360 h (as shown in Figure 12). Damage caused by the weathering cycle was assessed using visual assessment and gloss measurement.

The weatherability property of conventional alkyd-MF materials was observed to improve with incorporation of CNSL-based hybrid sol. The damage due to UV radiation was observed to decrease on increasing the content of CNSL-based hybrid sol. This could be attributed to more numbers of siloxane linkages in AM-50 formulation. The increased number of stronger Si-O bonds (bond dissociation energy of 190.73 Kcal/mol) in AM-50 formulation imparted enhanced UV resistance compared to the case of other formulations. The visual examination of the exposed specimen shows that AM-50 formulation showed excellent resistance against formation of corrosion products (pits) on the surface after UV exposure, as shown in Figure 12. The Gloss retention of the AM-30 and AM-50 formulation after 360 hrs was observed to be 77.91% and 82.52% respectively. The gloss retention values of neat and 15% formulation were unable to be measured due to formation of pits on the surface after exposure.

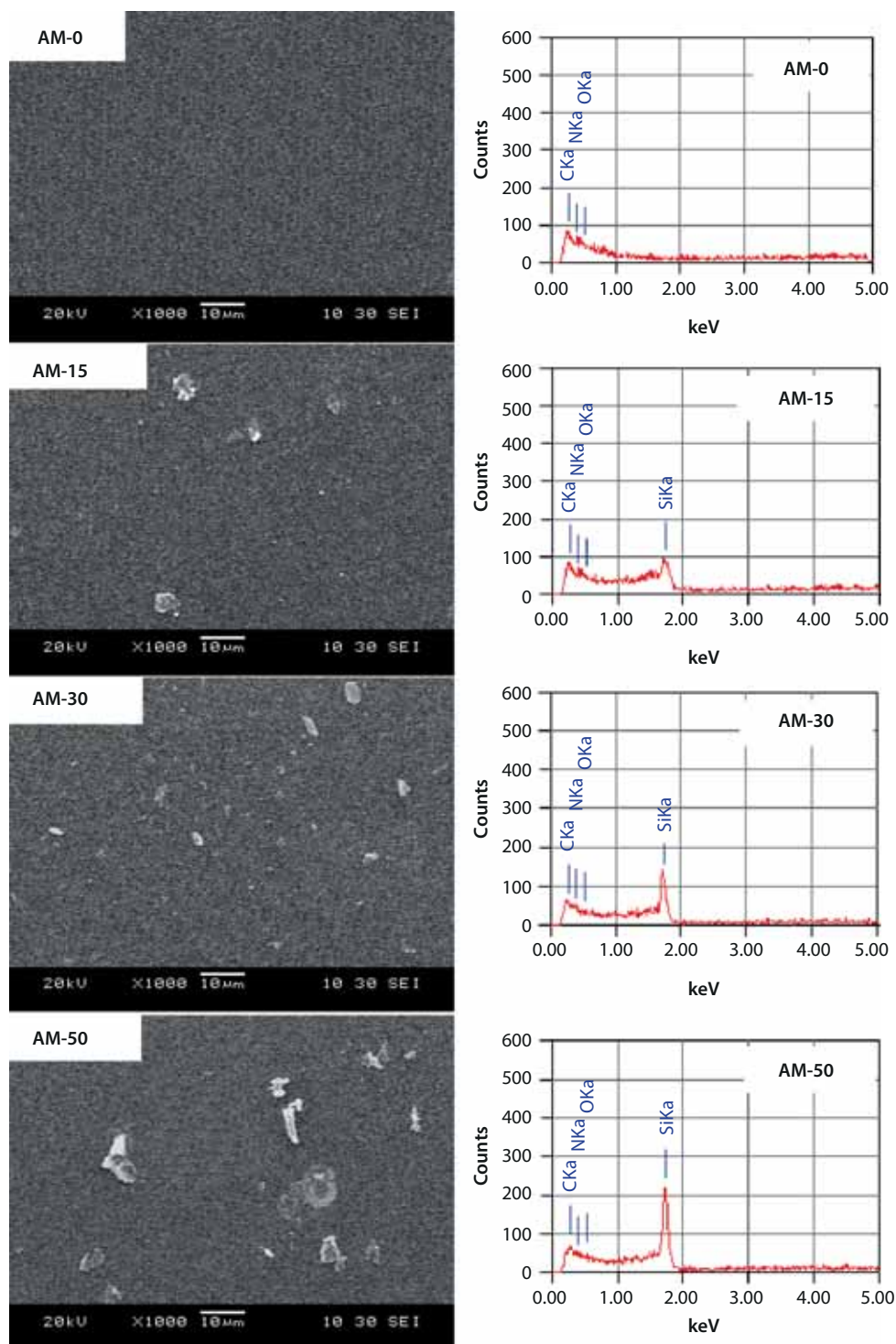
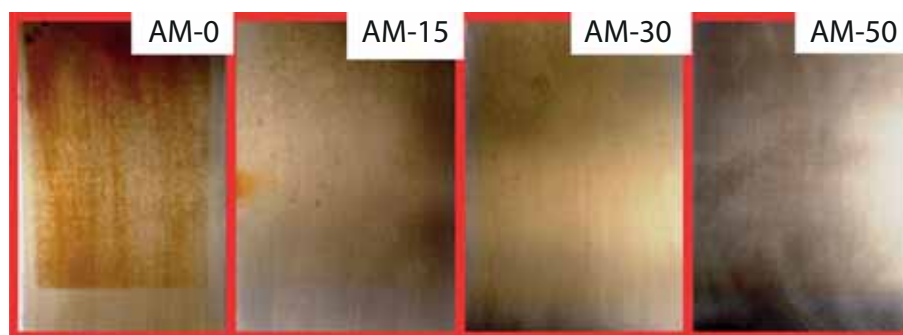


Figure 11 SEM/EDAX images of CNSL-based modified hybrid materials.

## 6 CONCLUSION

The effect of newly developed CNSL-based hybrid sol on the performance properties of conventional alkyd-MF system was studied. All mechanical properties

were observed to be similar for all the materials with an increasing trend in pencil hardness on increasing the content of hybrid sol, which could be due to increased crosslinking density. The formulation containing 50% of CNSL-based hybrid sol showed



**Figure 12** UV resistance of CNSL-based modified hybrid materials after 360 hrs of UV exposure with alternate UV and condensation cycles.

excellent performance in terms of chemical and solvent resistance properties. Silicone modification increased the corrosion resistance and UV stability of the system. Improvement in corrosion resistance is attributed to the formation of more siloxane linkages (Si-O-Si) at metal coating interface which are quite stable to aggressive environment. Furthermore, the combination of long-chain methylene linkages of CNSL and the presence of siloxane (Si-O-Si) moieties in the materials maintained the good balance between flexibility and hardness properties. On the basis of experimental results, we concluded that the developed CNSL-based hybrid sol can be successfully explored in conventional stoving system with improved performance.

## ACKNOWLEDGMENTS

The authors gratefully acknowledge Cardolite Corporation, Mangalore, and Shalimar Paints Ltd., Nashik, for their kind support in supplying raw materials and testing facilities respectively. Also, the authors would like to thank Nova Surface Care Centre Pvt. Ltd., Mumbai, for providing testing facilities.

## REFERENCES

1. T. Monetta, F. Bellucci, L. Nicodemo, and L. Nicolais, Protective properties of epoxy-based organic coatings on mild steel. *Prog. Org. Coat.* **21**, 353–369 (1993).
2. B. Bieganska, M. Zubielewicz, and E. Smieszek, Anticorrosive water-borne paints. *Prog. Org. Coat.* **15**, 33–56 (1987).
3. W.S. Araujo, I.C.P. Margarit, O.R. Mattos, and F.L. Fragata, Corrosion aspects of alkyd paints modified with linseed and soy oils. *Electrochim. Acta* **55**, 6204–6211 (2010).
4. L. Veleva, J. Chin, and B. Del Amo, Corrosion electrochemical behavior of epoxy anticorrosive paints based on zinc molybdenum phosphate and zinc oxide. *Prog. Org. Coat.* **36**(4), 211–216 (1999).
5. F. Cadena, L. Irusta, and M.J. Fernandez-Berridi, Performance evaluation of alkyd coatings for corrosion protection in urban and industrial environments. *Prog. Org. Coat.* **76**(9), 1273–1278 (2013).
6. A. Olad, M. Barati, and S. Behboudi, Preparation of PANI/epoxy/Zn nanocomposite using Zn nanoparticles and epoxy resin as additives and investigation of its corrosion protection behavior on iron. *Prog. Org. Coat.* **74**(1), 221–227 (2012).
7. G. Hernandez-Padron, F. Rojas, and V. Castano, Development and testing of anticorrosive SiO<sub>2</sub>/phenolic-formaldehydic resin coatings. *Surf. Coat. Technol.* **201**(3–4), 1207–1214 (2006).
8. M. Liu, X. Mao, H. Zhu, A. Lin, and D. Wang, Water and corrosion resistance of epoxy-acrylic-amine waterborne coatings: Effects of resin molecular weight, polar group and hydrophobic segment. *Corros. Sci.* **75**, 106–113 (2013).
9. K. Kowalczyk, K. Luczka, B. Grzmil, and T. Szychaj, Anticorrosive polyurethane paints with nano- and micro-sized phosphates. *Prog. Org. Coat.* **74**(1), 151–157 (2012).
10. T.S. Velayutham, W.H. Abd Majid, A.B. Ahmad, G.Y. Kang, and S.N. Gan, Synthesis and characterization of polyurethane coatings derived from polyols synthesized with glycerol, phthalic anhydride and oleic acid. *Prog. Org. Coat.* **66**(4), 367–371 (2009).
11. G. Parashar, D. Srivastava, and P. Kumar, Ethyl silicate binders for high performance coatings. *Prog. Org. Coat.* **42**(1–2), 1–14 (2001).
12. U.S. Department of Health and Human Services, Public Health Service, Agency for Toxic Substances and Disease Registry, Toxicological profile for Chromium. (2008) [www.atsdr.cdc.gov/toxprofiles/tp7.pdf](http://www.atsdr.cdc.gov/toxprofiles/tp7.pdf).
13. U.S. Environmental Protection Agency Washington, DC, Toxicological review of hexavalent chromium. (1998) <http://www.epa.gov/iris/toxreviews/0144tr.pdf>
14. D. Wang, and G.P. Bierwagen, Sol-gel coatings on metals for corrosion protection. *Prog. Org. Coat.* **64**, 327–338 (2009).
15. D.B. Balgude, and A.S. Sabnis, Sol-gel derived hybrid coatings as an environment friendly surface treatment for corrosion protection of metals and their alloys. *J. Sol-Gel Sci. Technol.* **64**, 124–134 (2012).

16. A.K. Mohanty, M. Misra, and G. Hinrichsen, Biofibres, biodegradable polymers and biocomposites: An overview. *Macromol. Mater. Eng.* **276/277**, 1–24 (2000).
17. F. Zafar, S.M. Ashraf, and S. Ahmad, Air drying polyesteramide from a sustainable resource. *Prog. Org. Coat.* **51**, 250–256 (2004).
18. X. Pan, P. Sengupta, and D.C. Webster, High biobased content epoxy-anhydride thermosets from epoxidized sucrose esters of fatty acids. *Biomacromol.* **12**(6), 2416–2428 (2011).
19. C.B. Ferrer, E. Hablot, M.C. Garrigos, S. Bocchini, L. Averous, and A. Jimenez, Relationship between morphology, properties and degradation parameters of novative biobased thermoplastic polyurethanes obtained from dimer fatty acids. *Polym. Degrad. Stab.* **97**, 1964–1969 (2012).
20. W.D. Oliveira, and W.G. Glasser, Multiphase materials with lignin. 11. Starlike copolymers with caprolactone. *Macromol.* **27**, 5–11 (1994).
21. Y. Li, J. Mlynar, and S. Sarkanen, The first 85% kraft lignin-based thermoplastics. *J. Polym. Sci. B: Polym. Phys.* **35**(12), 1899–1910 (1997).
22. N. Cordeiro, P. Aurenty, M.N. Belgacem, A. Gandini, and C.P. Neto, Surface Properties of Suberin *J. Colloid Interface Sci.* **187**, 498–508 (1997).
23. M. J. Dumont, X. Kong, and S. S. Narine, Polyurethanes from benzene polyols synthesized from vegetable oils: Dependence of physical properties on structure. *J. Appl. Polym. Sci.* **117**, 3196–3203 (2010).
24. D.B. Balgude, and A.S. Sabnis, CNSL: An environment friendly alternative for the modern coating industry. *J. Coat Technol Res.* **11**(2), 169–183 (2014).
25. D.B. Balgude, and A.S. Sabnis, *J. Polym. Mater.* **31**(3), 247–261 (2014).
26. D.B. Balgude, and A.S. Sabnis, *J. Renew. Mater.* **2**(3), 235–245 (2014).
27. D.B. Balgude, K.L. Konge, and A.S. Sabnis, Synthesis and characterization of sol-gel derived CNSL based hybrid anti-corrosive coatings. *J. Sol-Gel Sci. Technol.* **69**(1), 155–165 (2014).
28. N. Yasaharu, Maleinization process, US Patent 3778418, (1973).
29. G.R. Rossman, Vibrational spectroscopy of hydrous components. *Rev. Mineral* **18**, 193–206 (1988).
30. G. Gupta, S.S. Pathak, and A.S. Khanna, *Prog. Org. Coat.* **506**(74), 106–114 (2012).
31. D.L. Pavia, G.M. Lampman, G.S. Kriz, and J.R. Vyvyan, *Introduction to Spectroscopy*, 4th ed., Brooks/Cole, Cengage Learning Inc., United States (2009).
32. R.H. Glaser, G.L. Wilkes, and C.E. Bronnimann, Solid-state <sup>29</sup>Si NMR of TEOS-based multifunctional sol-gel materials. *J. Non-Cryst. Solids* **113**, 73–87 (1989).
33. L. Costa, and G. Camino, Thermal behaviour of melamine. *J. therm. Anal.* **34**, 423–429 (1988).
34. T.L. Metroke, O. Kachurina, and E.T. Knobbe, Spectroscopic and corrosion resistance characterization of GLYMO-TEOS Ormosil coatings for aluminum alloy corrosion inhibition. *Prog. Org. Coat.* **44**, 295–305 (2002).